Nearest-neighbor distribution for singular billiards

E. Bogomolny, O. Giraud, and C. Schmit
Laboratoire de Physique Théorique et Modèles Statistiques, Université de Paris XI, Bâtiment 100, 91405 Orsay Cedex, France
(Received 19 December 2001; published 17 May 2002)

The exact computation of the nearest-neighbor spacing distribution $P(s)$ is performed for a rectangular billiard with a pointlike scatterer inside for periodic and Dirichlet boundary conditions, and it is demonstrated that when $s\to\infty$ this function decreases exponentially. Together with the results of Bogomolny, Gerland, and Schmit [Phys. Rev. E **63**, 036206 (2001)], it proves that spectral statistics of such systems is of intermediate type characterized by level repulsion at small distances and exponential fall-off of the nearest-neighbor distribution at large distances. The calculation of the nth nearest-neighbor spacing distribution $P_n(s)$ and its asymptotics is performed as well for any boundary conditions.

DOI: 10.1103/PhysRevE.65.056214 PACS number(s): 05.45.−a, 03.65.Sq, 05.40.−a

I. INTRODUCTION

The statistical analysis of quantum energy levels for a given system in the semiclassical limit is a well-studied feature in the theory of spectral statistics [1–3]. The main conjectures in this field are as follows.

(i) The Berry-Tabor conjecture [4]: generic integrable systems obey Poisson statistics, which implies that their energy levels behave as independent random variables.

(ii) The Bohigas-Giannoni-Schmit conjecture [5]: generic chaotic systems follow the Wigner-Dyson distributions of random matrix theory (see [2]).

There is an enormous amount of numerical evidence that many physical systems do agree with these two main level statistics. Partial analytical results support these conjectures for integrable rectangular billiards [6] and quantum chaotic systems [7–10].

However, there exist systems which are neither integrable nor chaotic and their spectral statistics do not follow any of the above leading models. In many cases their statistics have features intermediate between the Poisson statistics and that of random matrix ensembles and for this reason they are called "intermediate statistics" [11–13]. For the first time this type of behavior was clearly observed numerically for the three-dimensional Anderson model at the metal-isolator transition point [11], and later it was argued [14] that spectral statistics of diffractive and pseudointegrable systems is also of intermediate type.

To study precisely the statistical behavior of the energy levels of quantum systems, one usually introduces different functions that characterize the statistics [2]. The most important quantity for our purpose is the distribution of nearest-neighbor spacings, $P(s)$, which is the probability that two levels are separated by a distance s with no levels inside this interval.

For the Poisson statistics, the nearest-neighbor distribution takes the following particularly simple form:

$$P(s)=\exp(-s) \tag{1}$$

and it is characterized by (i) the absence of level repulsion $[P(0)\neq 0]$ and (ii) exponential decay for a large distance.

For standard random matrix ensembles, the nearest-neighbor spacing distributions are given by complicated expressions [2] but their main features can be seen from the Wigner surmise,

$$P(s)=a_\beta s^\beta \exp(-c_\beta s^2), \tag{2}$$

where $\beta=1, 2$, and 4 corresponds, respectively, to orthogonal, unitary, or symplectic ensembles, and a_β and c_β are constants determined by the normalization conditions. Its main properties are (i) level repulsion, $P(0)=0$, and (ii) a very quick decrease at large values of s, $P(s)\propto\exp(-cs^2)$ when $s\to\infty$.

We call spectral statistics of intermediate type if they have the following hybrid properties (cf. [11,14]): (i) they exhibit the level repulsion, $P(0)=0$, as for standard random matrix ensembles, and (ii) they have exponential decay at large s, $P(s)\propto\exp(-cs)$ when $s\to\infty$, similarly to the Poisson statistics. Little is known analytically for systems with intermediate statistics, though it is possible to write down models which will have this type of statistics [15,12].

The rectangular billiard with a pointlike scatterer inside belongs to the class of diffractive systems and is one of the models which is supposed to have intermediate statistics [14,13]. Without the scatterer this model is an integrable system, and when the ratio a^2/b^2 of the sides of the rectangle is a "good" irrational number its quantum energy levels $\{e_n\}$ obey the Poisson statistics [4,6]. The addition of a δ-function scatterer

$$V=\lambda\,\delta(\vec{x}-\vec{x}_0) \tag{3}$$

inside the rectangle corresponds to a rank-1 perturbation, and the new quantum energy levels E of the perturbed rectangular billiard will obey the following quantization condition [16,17]:

$$\lambda\sum_n \frac{|\psi_n^{(0)}(\vec{x}_0)|^2}{E-e_n}=1, \tag{4}$$

where $\psi_n^{(0)}$ and e_n are the eigenfunctions and eigenvalues of the unperturbed rectangular billiard. Similar equations appear in different models. In particular, the quantization condition for the star graphs can be transformed to this form [18]. All our results are applicable without changes in such cases as well.

Rank-1 perturbations have been studied in the context of ballistic motion of particles in regular [17] or chaotic cavities [19], and in the context of random matrix theory [20]. When a δ-function potential (3) is added to a chaotic system with random matrix statistics, it has been proved [21] that the new eigenvalues in Eq. (4) are also distributed according to the same statistics. In the chaotic case, the universal part of the spectral statistics is not changed by finite-rank perturbation. On the contrary, when the unperturbed system is integrable, the perturbation (3) changes dramatically its spectral statistics [17,13].

In Ref. [13], the two-point correlation function of a rectangular billiard with a small-size scatterer inside [described by the potential (3)] has been computed analytically. One of the conclusions of this paper was that spectral statistics of such singular billiards do have level repulsion. For billiards with periodic boundary conditions, the two-point correlation function and, consequently, the nearest-neighbor distribution vanish linearly at small distances with the slope independent of the coupling constant,

$$P(s) \underset{s\to 0}{\sim} \frac{\pi\sqrt{3}}{2} s. \tag{5}$$

For billiards with Dirichlet boundary conditions, the small-s behavior of the two-point correlation function and the nearest-neighbor distribution is different: one has (see [13])

$$P(s) \underset{s\to 0}{\sim} \frac{1}{8\pi^3} s \ln^4 s. \tag{6}$$

The main purpose of this paper is to compute analytically the nearest-neighbor spacing distributions for this model and demonstrate that for any boundary conditions they decrease exponentially at large separation. Together with the results of Ref. [13] regarding the existence of level repulsion, it will furnish the proof that spectral statistics of these systems are of intermediate type.

The plan of the paper is as follows. In Sec. II, we generalize the formalism used in [13] to describe the nearest-neighbor spacing distribution for a billiard with a pointlike scatterer for periodic and Dirichlet boundary conditions. Though the resulting formulas are explicit and exact, they are quite cumbersome, and in Sec. III we study the asymptotic behavior of $P(s)$ for large s. It is demonstrated that in all cases the nearest-neighbor distribution has an exponential tail at large distances thus proving the intermediate character of the spectral statistics of singular billiards. In Sec. IV, the nth nearest-neighbor spacing distributions for these billiards with periodic and Dirichlet boundary conditions are computed analytically and their large distance asymptotics are found as well. In the Appendix, we present certain technical details of the computation of necessary integrals.

II. THE GENERAL FORMALISM

A. Preliminary computations

In this section, our aim is to find analytical expressions for the nearest-neighbor spacing distribution of the solutions, E, of the following equation:

$$\lambda \sum_{j=1}^{N} \frac{r_j}{E-e_j} = 1, \tag{7}$$

where e_j, $j=1,\ldots,N$ are independent random variables with a uniform distribution $d\mu(e)$:

$$d\mu(e) = \begin{cases} \dfrac{1}{2W} de & \text{if } -W \leqslant e \leqslant W \\ 0 & \text{otherwise,} \end{cases} \tag{8}$$

and r_j are positive constants with mean value 1,

$$\frac{1}{N} \sum_{n=1}^{N} r_n = 1. \tag{9}$$

This normalization condition permits us to introduce conveniently the coupling constant λ.

In general, this equation describes zeros of a meromorphic function whose poles are assumed to be independent random variables, and it can correspond to different physical problems (see, e.g., [22]). In this paper, we prefer to consider it as the quantization condition of rectangular (or more general integrable) billiards with a small-size impurity inside [16,17]. To ensure that energy levels of unperturbed billiards behave as independent random variables, it is necessary to assume that the ratio of squares of the sides of the rectangle, a and b, is an irrational number badly approximated by a rational (that is, a diophantine number) [6] with the following property:

$$\left| \frac{a^2}{b^2} - \frac{m}{n} \right| > \frac{C}{n^k} \tag{10}$$

for all integers m, n, and some $k \geqslant 2$.

The residues, r_n, depend on boundary conditions. For quantum problems with periodic boundary conditions, $r_n = 1$. For Dirichlet conditions,

$$r_{mn} = 4 \sin^2\left(\frac{\pi}{a} m x_0\right) \sin^2\left(\frac{\pi}{b} n y_0\right), \tag{11}$$

where x_0, y_0 are coordinates of the singular scatterer. When the ratios x_0/a and y_0/b are noncommensurable irrational numbers and $m,n \to \infty, r_{mn}$ can be considered as independent random variables,

$$r_{mn} = 4 \sin^2 \phi_1 \sin^2 \phi_2 \tag{12}$$

with angles ϕ_i uniformly distributed between 0 and $\pi/2$.

When both ratios x_0/a and y_0/b are rational numbers,

$$\frac{x_0}{a}=\frac{p_1}{q_1}, \qquad \frac{y_0}{b}=\frac{p_2}{q_2} \tag{13}$$

with coprime integers (p_i,q_i), the residues (11) only depend on m mod q_1 and n mod q_2 and there is only a finite number of residues determined by q_i angles ϕ_i in Eq. (12) (see [13] for more detail),

$$\phi_1=\pi\frac{k_1}{q_1} \text{ with } k_1=0,1,\ldots,q_1-1,$$

$$\phi_2=\pi\frac{k_2}{q_2} \text{ with } k_2=0,1,\ldots,q_2-1. \tag{14}$$

All our formulas below remain valid for general r_n.

Obviously there are N solutions E_j of Eq. (7) since each interval $]e_i,e_{i+1}[$ contains one and only one of these solutions. We are interested in the nearest-neighbor distribution, $P(s)$, that is the probability that two energy levels E_i and E_j are neighbors separated by a distance s. In our case, it is the probability that two solutions E_i and E_j of Eq. (7) are separated by one and only one unperturbed level e_k, and that $|E_i-E_j|=s$. Let us compute at first the probability $P(E_1,E_2)$ that two given energy levels E_1 and E_2 are neighbors. Assuming for instance that $E_2<E_1$, $P(E_1,E_2)$ is the probability that that one solution of Eq. (7) equals E_1, another one equals E_2, and that there exists $i, 1\leqslant i\leqslant N$, such that

$$e_i\in]E_2,E_1[, \quad \forall\ j\neq i, \quad e_j\notin]E_2,E_1[. \tag{15}$$

As it is supposed that e_k are independent random variables with a uniform distribution,

$$P(E_1,E_2)=\int_{-W}^{W}\prod_{k=1}^{N}\frac{de_k}{2W}\rho(E_1)\rho(E_2) \times\sum_{i=1}^{N}\chi(e_i)\prod_{j\neq i}[1-\chi(e_j)], \tag{16}$$

where $\chi(e)$ is the characteristic function of the interval $]E_2,E_1[$ equal to 1 if e belongs to $]E_2,E_1[$, and to 0 otherwise, and ρ is the density of the solutions E_i,

$$\rho(E)=\sum_{i=1}^{N}\delta(E-E_i). \tag{17}$$

It is convenient to rewrite these formulas in a more symmetric way,

$$P(E_1,E_2)=\sum_{\{\sigma_k\}}\int\prod_{k=1}^{N}d\mu_{\sigma_k}(e_k)\rho(E_1)\rho(E_2), \tag{18}$$

where variables σ_k, $k=1,\ldots,N$ take two values, 0,1, and we introduce two different measures,

$$\int d\mu_0(e)\phi(e)=\frac{1}{2W}\int_{-W}^{W}\chi(e)\phi(e)de =\frac{1}{2W}\int_{E_2}^{E_1}\phi(e)de \tag{19}$$

and

$$\int d\mu_1(e)\phi(e)=\frac{1}{2W}\int_{-W}^{W}[1-\chi(e)]\phi(e)de =\frac{1}{2W}\left(\int_{-W}^{W}-\int_{E_2}^{E_1}\right)\phi(e)de. \tag{20}$$

The summation in Eq. (18) is performed over all sequences σ_k which contain one zero and $N-1$ ones.

Because $\{E_i\}$ are solutions of Eq. (7), the density of states (17) can be rewritten under the form (cf. [13])

$$\rho(E)=\delta\left(\sum_{i=1}^{N}\frac{r_j}{E-e_j}-\frac{1}{\lambda}\right)\sum_{k=1}^{N}\frac{r_k}{(E-e_k)^2}. \tag{21}$$

Representing the δ function by a Fourier integral, one gets

$$\rho(E)=\int_{-\infty}^{\infty}\frac{d\alpha}{2\pi}\exp\left[i\alpha\left(\sum_{i=1}^{N}\frac{r_j}{E-e_j}-\frac{1}{\lambda}\right)\right] \times\sum_{k=1}^{N}\frac{r_k}{(E-e_k)^2} \tag{22}$$

and finally the probability (16) can be put under the form

$$P(E_1,E_2)=\int_{-\infty}^{\infty}\frac{d\alpha_1 d\alpha_2}{4\pi^2}\sum_{\{\sigma_k\}}\int\prod_{k=1}^{N}d\mu_{\sigma_k}(e_k)e^{-i(\alpha_1+\alpha_2)/\lambda} \times\sum_{k_1,k_2=1}^{N}\frac{r_{k_1}r_{k_2}}{(E_1-e_{k_1})^2(E_2-e_{k_2})^2} \times\prod_{j_1,j_2=1}^{N}\exp\left(i\alpha_1\frac{r_{j_1}}{E_1-e_{j_1}}+i\alpha_2\frac{r_{j_2}}{E_2-e_{j_2}}\right). \tag{23}$$

Let us introduce the following functions:

$$f_\sigma(\alpha_1,\alpha_2)=\int d\mu_\sigma(e)\exp\left(i\frac{\alpha_1}{E_1-e}+i\frac{\alpha_2}{E_2-e}\right),$$

$$\Psi_{j\sigma}(\alpha_1,\alpha_2)=\int d\mu_\sigma(e)\frac{1}{(E_j-e)^2} \times\exp\left(i\frac{\alpha_1}{E_1-e}+i\frac{\alpha_2}{E_2-e}\right),$$

$$g_\sigma(\alpha_1,\alpha_2)=\int d\mu_\sigma(e)\frac{1}{(E_1-e)^2(E_2-e)^2} \times\exp\left(i\frac{\alpha_1}{E_1-e}+i\frac{\alpha_2}{E_2-e}\right). \tag{24}$$

The nearest-neighbor distribution can be expressed through these functions in the following way:

$$P(E_1,E_2)=\sum_{\{\sigma_k\}}\int_{-\infty}^{\infty}\frac{d\alpha_1 d\alpha_2}{4\pi^2}\left(\sum_j r_j^2 g_{\sigma_j}(\alpha r_j)\prod_{k\neq j} f_{\sigma_k}(\alpha r_k)+\sum_{j\neq k} r_j r_k \Psi_{1\sigma_j}(\alpha r_j)\Psi_{2\sigma_k}(\alpha r_k)\prod_{l\neq j,k} f_{\sigma_l}(\alpha r_l)\right)e^{-i(\alpha_1+\alpha_2)/\lambda}. \quad (25)$$

Here and below when it will not lead to a confusion we use the notation $f(\alpha)$ for a function of two variables $f(\alpha_1,\alpha_2)$ and $f(\alpha r)$ instead of $f(\alpha_1 r,\alpha_2 r)$. This formula is valid for all sequences of σ_k. The functions (24) with index $\sigma=0$ correspond to an unperturbed level between E_2 and E_1, and the functions with index $\sigma=1$ correspond to an unperturbed level outside $]E_2,E_1[$. Therefore, to describe the nearest-neighbor distribution, the summation should be done over N possible sequences containing only one zero.

The functions $\Psi_{j\sigma}$ and g_σ are related to f_σ by the relations

$$\Psi_{j\sigma}(\alpha_1,\alpha_2)=-\frac{\partial^2}{\partial\alpha_j^2}f_\sigma(\alpha_1,\alpha_2), g_\sigma(\alpha_1,\alpha_2)=\frac{\partial^4}{\partial\alpha_1^2\partial\alpha_2^2}f_\sigma(\alpha_1,\alpha_2). \quad (26)$$

Therefore, in order to compute $P(E_1,E_2)$ it is necessary to find only f_σ. Let us introduce the functions

$$I_\sigma(\alpha_1,\alpha_2)=2W\int d\mu_\sigma(e)\left[1-\exp\left(i\frac{\alpha_1}{E_1-e}+i\frac{\alpha_2}{E_2-e}\right)\right], \quad (27)$$

which are related to our basic functions f_σ as follows:

$$f_1(\alpha_1,\alpha_2)=1-\frac{\omega}{2W}-\frac{1}{2W}I_1(\alpha_1,\alpha_2),$$

$$f_0(\alpha_1,\alpha_2)=\frac{\omega}{2W}-\frac{1}{2W}I_0(\alpha_1,\alpha_2), \quad (28)$$

where $\omega=E_1-E_2$ is the difference of energies (we recall that we have assumed $E_2<E_1$).

The integral defining $I_1(\alpha)$ can be split into two parts,

$$I_1(\alpha_1,\alpha_2)=\left(\int_{-W}^{E_2}+\int_{E_1}^{W}\right)\times\left[1-\exp\left(i\frac{\alpha_1}{E_1-e}+i\frac{\alpha_2}{E_2-e}\right)\right]de =J_1(\alpha_1,\alpha_2)+j(\alpha_1,\alpha_2), \quad (29)$$

where

$$J_1(\alpha_1,\alpha_2)=\left(\int_{-\infty}^{E_2}+\int_{E_1}^{\infty}\right)\times\left[1-\exp\left(i\frac{\alpha_1}{E_1-e}+i\frac{\alpha_2}{E_2-e}\right)\right]de \quad (30)$$

and

$$j(\alpha_1,\alpha_2)=-\left(\int_{-\infty}^{-W}+\int_{W}^{\infty}\right)\times\left[1-\exp\left(i\frac{\alpha_1}{E_1-e}+i\frac{\alpha_2}{E_2-e}\right)\right]de. \quad (31)$$

For convenience, we define the function $J_0(\alpha)=I_0(\alpha)$ so that from Eq. (27)

$$J_0(\alpha_1,\alpha_2)=\int_{E_2}^{E_1}\left[1-\exp\left(i\frac{\alpha_1}{E_1-e}+i\frac{\alpha_2}{E_2-e}\right)\right]de. \quad (32)$$

The integral (31) defining $j(\alpha)$ has no singularity inside the integration region, and as was demonstrated in [13], it is sufficient to take into account only terms linear in α and to ignore the difference between E_1 and E_2 (i.e., set $E_1\approx E_2\approx E$). In this approximation,

$$j(\alpha_1,\alpha_2)=i(\alpha_1+\alpha_2)\ln\frac{W-E}{W+E}. \quad (33)$$

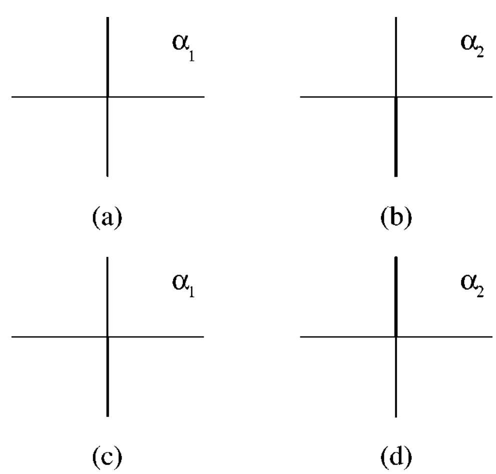

FIG. 1. The cuts in complex planes of α_1 and α_2 for functions $\tilde{J}_1$ and ϕ_1 (a),(b); $\tilde{J}_0$ and ϕ_0 (c),(d).

On the contrary, the functions $J_\sigma(\alpha)$ are quite cumbersome. One can easily check that they depend only on the difference of energies, $\omega = E_1 - E_2$, and that

$$J_\sigma(\alpha) = \omega \tilde{J}_\sigma\left(\frac{\alpha}{\omega}\right), \tag{34}$$

where the functions $\tilde{J}_\sigma(\alpha)$ are defined by Eqs. (30) and (32) with $E_1 = 1$ and $E_2 = 0$.

In the Appendix, it is demonstrated that these functions obey the differential equation

$$(\partial_1 - \partial_2)\tilde{J}_\sigma(\alpha_1,\alpha_2) = e^{i(\alpha_1-\alpha_2)}\phi_\sigma(\alpha_1,\alpha_2), \tag{35}$$

where ∂_i denotes the derivative with respect to α_i, and the functions $\phi_\sigma(\alpha)$ at real α are given by Eqs. (A7) and (A10). From this equation it follows (see the Appendix for details) that the function $\tilde{J}_1(\alpha)$ is an analytical function of two complex variables α_1, α_2 with the cuts as in Figs. 1(a) and 1(b) given by the following expression:

$$\tilde{J}_1(\alpha_1,\alpha_2) = \fint_{-1}^{\infty}\frac{dt}{t^2}(1 - e^{i(\alpha_1+\alpha_2)t}) + \int_0^{\alpha_1} e^{i(2t-\alpha_1-\alpha_2)}\phi_1(t,\alpha_1+\alpha_2-t)\,dt, \tag{36}$$

where $\fint$ denotes the principal part of the integral.

The function $\tilde{J}_0(\alpha)$ is an analytical function in a region indicated in Figs. 1(c) and 1(d) with the integral representation

$$\tilde{J}_0(\alpha_1,\alpha_2) = \int_1^{\infty}\frac{dt}{t^2}(1 - e^{-i(\alpha_1+\alpha_2)t}) + \int_0^{\alpha_1} e^{i(2t-\alpha_1-\alpha_2)}\phi_0(t,\alpha_1+\alpha_2-t)\,dt. \tag{37}$$

Exactly as was done in [13], one can prove that functions $\Psi_{i\sigma}, g_\sigma$ defined in Eqs. (24) can be expressed through the functions ϕ_σ as follows:

$$g_\sigma(\alpha_1,\alpha_2) = \frac{1}{2W\omega^2}(\partial_1 - \partial_2)\left[e^{i[(\alpha_1-\alpha_2)/\omega]}\phi_\sigma\left(\frac{\alpha_1}{\omega},\frac{\alpha_2}{\omega}\right)\right],$$

$$\Psi_{1\sigma}(\alpha_1,\alpha_2) = \frac{1}{2W}e^{i[(\alpha_1-\alpha_2)/\omega]}\partial_1\phi_\sigma\left(\frac{\alpha_1}{\omega},\frac{\alpha_2}{\omega}\right),$$

$$\Psi_{2\sigma}(\alpha_1,\alpha_2) = -\frac{1}{2W}e^{i[(\alpha_1-\alpha_2)/\omega]}\partial_2\phi_\sigma\left(\frac{\alpha_1}{\omega},\frac{\alpha_2}{\omega}\right). \tag{38}$$

B. Nearest-neighbor spacing distribution

Using Eqs. (38), one can integrate the first term in Eq. (25) by parts and because [see Eqs. (28) and (34)]

$$(\partial_1 - \partial_2)f_\sigma(\alpha_1,\alpha_2) = -\frac{1}{2W}e^{i(\alpha_1-\alpha_2)/\omega}\phi_\sigma\left(\frac{\alpha_1}{\omega},\frac{\alpha_2}{\omega}\right) \tag{39}$$

one obtains

$$\int_{-\infty}^{\infty}\frac{d\alpha_1 d\alpha_2}{4\pi^2}\sum_j r_j^2 g_{\sigma_j}(\alpha r_j)\left(\prod_{k\neq j} f_{\sigma_k}(\alpha r_k)\right)e^{-i(\alpha_1+\alpha_2)/\lambda} = \frac{1}{\omega^2(2W)^2}\int_{-\infty}^{\infty}\frac{d\alpha_1 d\alpha_2}{4\pi^2}\sum_{j\neq k} r_j r_k \phi_{\sigma_j}\left(\frac{\alpha}{\omega}r_j\right)\phi_{\sigma_k}\left(\frac{\alpha}{\omega}r_k\right)e^{i[(\alpha_1-\alpha_2)/\omega](r_k+r_j)} \times\left(\prod_{l\neq j,k} f_{\sigma_l}(\alpha r_l)\right)e^{-i(\alpha_1+\alpha_2)/\lambda}. \tag{40}$$

According to Eqs. (38), the second term in Eq. (25) can also be expressed through the same functions $\phi_\sigma(\alpha)$, and after the scaling of variables $\alpha \to \alpha\omega$ [cf. Eq. (34)] the nearest-neighbor distribution (25) takes the form

$$P(\omega) = \sum_{\{\sigma_k\}}\int_{-\infty}^{\infty}\frac{d\alpha_1 d\alpha_2}{(4W\pi)^2}\sum_{j\neq k} r_j r_k\{\phi_{\sigma_j}(\alpha r_j)\phi_{\sigma_k}(\alpha r_k) - \partial_1\phi_{\sigma_j}(\alpha r_j)\partial_2\phi_{\sigma_k}(\alpha r_k)\}e^{i(\alpha_1-\alpha_2)(r_j+r_k)} \times\left(\prod_{l\neq j,k}\tilde{f}_{\sigma_l}(\alpha r_l)\right)e^{-i\omega(\alpha_1+\alpha_2)/\lambda}, \tag{41}$$

where $\tilde{f}_{\sigma_l}(\alpha) = f_{\sigma_l}(\alpha\omega)$. Using Eqs. (28), (29), and (31), one gets

$$\tilde{f}_1(\alpha_1,\alpha_2) = 1 - \frac{\omega}{2W}\left(1 + \tilde{J}_1(\alpha_1,\alpha_2) + i(\alpha_1+\alpha_2)\ln\frac{W-E}{W+E}\right),$$

$$\tilde{f}_0(\alpha_1,\alpha_2) = \frac{\omega}{2W}[1 - \tilde{J}_0(\alpha_1,\alpha_2)]. \tag{42}$$

Expression (41) is valid for any sequence $\{\sigma_k\}\in\{0,1\}^N$. To get the nearest-neighbor distribution, one has to sum over N sequences containing only one zero. Taking into account that in the limit $N\to\infty$ the restriction $j\neq k$ is unessential, we obtain, keeping only the dominant term,

$$P(\omega)=\frac{N^2}{4W^2}\int_{-\infty}^{\infty}\frac{d\alpha_1 d\alpha_2}{(2\pi)^2}[N\langle\tilde{f}_0(\alpha r)\rangle V_{\phi_1,\phi_1}(\alpha)+V_{\phi_0,\phi_1}(\alpha)+V_{\phi_1,\phi_0}(\alpha)]\times\left(\prod_l \tilde{f}_1(\alpha r_l)\right)e^{-i\omega(\alpha_1+\alpha_2)/\lambda}, \tag{43}$$

where the operator $V_{f,g}(\alpha)$ is defined for arbitrary functions $f(\alpha)$ and $g(\alpha)$ by the following expression:

$$V_{f,g}(\alpha)=\langle rf(\alpha r)e^{i(\alpha_1-\alpha_2)r}\rangle\langle rg(\alpha r)e^{i(\alpha_1-\alpha_2)r}\rangle-\left\langle\left(\frac{\partial}{\partial\alpha_1}f(\alpha r)\right)e^{i(\alpha_1-\alpha_2)r}\right\rangle\times\left\langle\left(\frac{\partial}{\partial\alpha_2}g(\alpha r)\right)e^{i(\alpha_1-\alpha_2)r}\right\rangle, \tag{44}$$

and $\langle f(r)\rangle$ means the mean value over all values of r,

$$\langle f(r)\rangle=\frac{1}{N}\sum_{n=1}^{N}f(r_n). \tag{45}$$

Measuring the energy difference ω in the units of mean level spacing

$$s=\frac{N\omega}{2W}, \tag{46}$$

the product $\Pi_l\tilde{f}_1(\alpha r_l)$ can also be simplified in the limit of large N [see Eq. (42)],

$$\prod_{l=1}^{N}\tilde{f}_1(\alpha r_l)\approx\exp\left[-\frac{N\omega}{2W}\left(1+\tilde{J}_1(\alpha_1,\alpha_2)+i(\alpha_1+\alpha_2)\ln\frac{W-E}{W+E}\right)\right]. \tag{47}$$

Introducing the renormalized coupling constant λ',

$$\frac{1}{\lambda'}=\frac{2W}{N\lambda}+\ln\frac{W-E}{W+E}, \tag{48}$$

we obtain the final formula for the nearest-neighbor distribution $P(s)=(2W/N)^2P(\omega)$,

$$P(s)=e^{-s}\int_{-\infty}^{\infty}\frac{d\alpha_1 d\alpha_2}{(2\pi)^2}\{s[1-\langle\tilde{J}_0(\alpha r)\rangle]V_{\phi_1,\phi_1}(\alpha)+V_{\phi_0,\phi_1}(\alpha)+V_{\phi_1,\phi_0}(\alpha)\}e^{-s[\langle\tilde{J}_1(\alpha r)\rangle+i(\alpha_1+\alpha_2)/\lambda']}. \tag{49}$$

C. Analytical continuation

Usually, if one wants to compute an integral

$$\int_{-\infty}^{\infty}d\alpha_1 d\alpha_2 f(\alpha_1,\alpha_2)e^{-sJ(\alpha_1,\alpha_2)}, \tag{50}$$

where $J(\alpha)$ and $f(\alpha)$ are analytical functions in a certain region, the first step is to move the integration contour as far as possible to decrease the integrand. In general, during that deformation one can either meet a saddle point or a singularity which signifies that further deformation of the contour either will increase the integrand or is not possible. If no such obstacle appears, the integral is zero.

In the case of the nearest-neighbor distribution (49), the saddle-point equation reads (taking here $r=1$)

$$\frac{\partial}{\partial\alpha_1}\tilde{J}_1(\alpha_1,\alpha_2)+\frac{i}{\lambda'}=0,\quad \frac{\partial}{\partial\alpha_2}\tilde{J}_1(\alpha_1,\alpha_2)+\frac{i}{\lambda'}=0. \tag{51}$$

In particular, these equations imply that at any saddle point,

$$\left(\frac{\partial}{\partial\alpha_1}-\frac{\partial}{\partial\alpha_2}\right)\tilde{J}_1(\alpha_1,\alpha_2)=0. \tag{52}$$

From Eqs. (A4) and (A6) it follows that this difference is proportional to $K_0(x)$ with $x=2\sqrt{\alpha_1\alpha_2}$. But $K_0(x)$ has no zero on the complex plane (see [23], p. 62). Therefore, our integral (49) has no saddle points and one can move the contour of integration freely. If the prefactor in (50) has no singularities in the region where $\tilde{J}_1$ is analytical, the contribution vanishes. Note that it is exactly what should be expected for physical reasons: replacing the prefactor in Eq. (49) by 1, we have to obtain the probability that there are two perturbed levels in E_2 and E_1 but no unperturbed energy levels between, which according to Eq. (7) is impossible. These considerations prove that the integral (49) with a prefactor equal to 1 or, more generally, with any prefactor analytical in the same domain as $\tilde{J}_1(\alpha)$ (and not too quickly increasing on infinity) must vanish.

These arguments allow us to simplify considerably the expression (49) for the nearest-neighbor distribution. The prefactor in Eq. (49) is

$$f(\alpha)=s[1-\langle\tilde{J}_0(\alpha r)\rangle]V_{\phi_1,\phi_1}(\alpha)+V_{\phi_0,\phi_1}(\alpha)+V_{\phi_1,\phi_0}(\alpha). \tag{53}$$

First, as only the functions with index 0 have analytical properties different from that of $\tilde{J}_1(\alpha)$ (see Fig. 1), one can drop the first term and keep only

$$f(\alpha)=-s\langle\tilde{J}_0(\alpha r)\rangle V_{\phi_1,\phi_1}(\alpha)+V_{\phi_0,\phi_1}(\alpha)+V_{\phi_1,\phi_0}(\alpha). \tag{54}$$

Secondly, according to Eqs. (A11) and (A21),

$$\phi_0(\alpha)=-\phi_1(\alpha)+\pi[\mathrm{sgn}(\alpha_1)-\mathrm{sgn}(\alpha_2)]J_0(2\sqrt{-\alpha_1\alpha_2}) \tag{55}$$

and

$$\tilde{J}_0(\alpha) = -\tilde{J}_1(\alpha) + \mathrm{sgn}(\alpha_1)R(\alpha) + \mathrm{sgn}(\alpha_2)R^\dagger(\alpha), \tag{56}$$

where the function $R(\alpha)$ is defined in Eq. (A22) and $R^\dagger(\alpha) = R^*(\alpha_2, \alpha_1)$.

When these expressions are substituted in Eq. (54), the terms with index 1 can be dropped out because they have the same analytical properties as $\tilde{J}_1(\alpha)$ and, as has been discussed above, their integrals vanish. Finally, the prefactor takes the form

$$f(\alpha) = -s[\mathrm{sgn}(\alpha_1)\langle R(\alpha r)\rangle + \mathrm{sgn}(\alpha_2)\langle R^\dagger(\alpha r)\rangle]V_{\phi_1,\phi_1}(\alpha) + \pi[\mathrm{sgn}(\alpha_1) - \mathrm{sgn}(\alpha_2)][V_{J_0,\phi_1}(\alpha) + V_{\phi_1,J_0}(\alpha)]$$
$$+ 2\pi i \frac{\delta(\alpha_1)}{\alpha_2 + i\epsilon}(\langle e^{-i\alpha_2 r}\rangle)^2 - 2\pi i \frac{\delta(\alpha_2)}{\alpha_1 - i\epsilon}(\langle e^{i\alpha_1 r}\rangle)^2, \tag{57}$$

where J_0 is the Bessel function $J_0(2\sqrt{-\alpha_1\alpha_2})$. The last term in this equation appears from the differentiation of $[\mathrm{sgn}(\alpha_1) - \mathrm{sgn}(\alpha_2)]$ in Eq. (44). The resulting δ function allows us to take the remaining terms at small α. We also write $\alpha_{1,2} \mp i\epsilon$, where $\epsilon \to 0^+$, to recall the region where the functions are defined.

When this expression is substituted in Eq. (49) one gets the final formula for the nearest-neighbor distribution, which can be conveniently written as a sum of three terms,

$$P(s) = \frac{e^{-s}}{4\pi^2}[A(s) + B(s) + C(s)], \tag{58}$$

where

$$A(s) = -s\int_0^\infty d\alpha_1 \int_{-\infty}^\infty d\alpha_2 \langle R(\alpha r)\rangle V_{\phi_1,\phi_1}(\alpha) e^{-s[\langle \tilde{J}_1(r\alpha)\rangle + i(\alpha_1+\alpha_2)/\lambda']}$$
$$-s\int_0^\infty d\alpha_2 \int_{-\infty}^\infty d\alpha_1 \langle R^\dagger(\alpha r)\rangle V_{\phi_1,\phi_1}(\alpha) e^{-s[\langle \tilde{J}_1(r\alpha)\rangle + i(\alpha_1+\alpha_2)/\lambda']} + \text{c.c.}, \tag{59}$$

$$B(s) = \pi\int_0^\infty d\alpha_1 \int_{-\infty}^\infty d\alpha_2 [V_{\phi_1,J_0}(\alpha) + V_{J_0,\phi_1}(\alpha)] e^{-s[\langle \tilde{J}_1(r\alpha)\rangle + i(\alpha_1+\alpha_2)/\lambda']} - \pi\int_0^\infty d\alpha_2 \int_{-\infty}^\infty d\alpha_1 [V_{\phi_1,J_0}(\alpha)$$
$$+ V_{J_0,\phi_1}(\alpha)] e^{-s[\langle \tilde{J}_1(r\alpha)\rangle + i(\alpha_1+\alpha_2)/\lambda']} + \text{c.c.}, \tag{60}$$

and

$$C(s) = 2\pi i \int_{-\infty}^\infty \frac{d\alpha_2}{\alpha_2 + i\epsilon}(\langle e^{-i\alpha_2 r}\rangle)^2 e^{-s[\langle \tilde{J}_1(0,r\alpha_2)\rangle + i\alpha_2/\lambda']} - 2\pi i \int_{-\infty}^\infty \frac{d\alpha_1}{\alpha_1 - i\epsilon}(\langle e^{i\alpha_1 r}\rangle)^2 e^{-s[\langle \tilde{J}_1(r\alpha_1,0)\rangle + i\alpha_1/\lambda']}. \tag{61}$$

These expressions look quite complicated, but in the next section we show that their asymptotics when $s \to \infty$ can easily be computed.

III. ASYMPTOTIC BEHAVIOR

The formulas (58)–(61) have been written in such a way that when the integration is performed from $-\infty$ to $+\infty$, the contour of integration as a whole can be shifted into the complex plane. The direction of such a deformation is different for the integration over α_1 and that over α_2. It can conveniently be fixed by the following change of variables: $\alpha_1 = -iv$ or $\alpha_2 = iv$. In the new variable the allowed deformation of the contour is in both cases $\mathrm{Re}\, v > 0$.

Let us consider first the simple integral (61). From Eqs. (A17) and (A23) of the Appendix it follows that $\tilde{J}_1(0,iv) = \tilde{J}_1(-iv,0) = I(v)$, where

$$I(v) = \int\!\!\!\!\!\!- _{-1}^{\infty} \frac{dt}{t^2}(1 - e^{-vt}) = e^v - 1 - v\,\mathrm{Ei}(v), \tag{62}$$

and

$$\mathrm{Ei}(v) = -\int\!\!\!\!\!\!- _{-v}^{\infty} \frac{dt}{t} e^{-t} \tag{63}$$

is the standard exponential integral (see, e.g., [23], p. 143).

Consequently, after the above change of variables the integral (61) takes the form

$$C(s)=-2\pi i\int_{-i\infty}^{+i\infty}\frac{dv}{v}(\langle e^{vr}\rangle)^2 e^{-s[\langle I(vr)\rangle - v/\lambda']}$$
$$-2\pi i\int_{-i\infty}^{+i\infty}\frac{dv}{v}(\langle e^{vr}\rangle)^2 e^{-s[\langle I(vr)\rangle + v/\lambda']}. \quad (64)$$

Now one can move the contour to the right until it goes through the saddle point. For the first integral, the position of the saddle point, v_+, is defined by the equation

$$\frac{d}{dv}\langle I(v_+ r)\rangle = \frac{1}{\lambda'} \quad (65)$$

and for the second integral the saddle point v_- is determined from a similar equation but with changed sign of the coupling constant λ',

$$\frac{d}{dv}\langle I(vr)\rangle = -\frac{1}{\lambda'}. \quad (66)$$

As $I'(v)=-\mathrm{Ei}(v)$, the saddle points $v_\pm$ are roots of the equation

$$\langle r\mathrm{Ei}(v_\pm r)\rangle = \mp\frac{1}{\lambda'} \quad (67)$$

and it is possible to prove that for any real λ' there is one and only one solution of this equation.

Expanding the exponent in Eq. (64) in the vicinity of the saddle points and taking into account that $I''(v)=-e^v/v$ and $\langle I(rv_\pm)\rangle \mp v_\pm/\lambda' = \langle e^{rv_\pm}\rangle - 1$, one gets that in the limit $s\to\infty$ the function (61) is the sum of contributions from two saddle points,

$$C(s)=(2\pi)^{3/2}\sum_{i=\pm}\frac{(\langle e^{rv_i}\rangle)^2}{\sqrt{\langle re^{rv_i}\rangle s v_i}}e^{-s(\langle e^{rv_i}\rangle -1)}. \quad (68)$$

The saddle point with the smallest value of $\langle e^{rv}\rangle$, which we denote by v_{sp}, dominates and it should formally be the only one to be taken into account. For finite λ', it corresponds to the solution of Eq. (67) with a negative right-hand side,

$$\langle r\mathrm{Ei}(rv_{\mathrm{sp}})\rangle = -\frac{1}{|\lambda'|}. \quad (69)$$

Note the appearance of the absolute value of the renormalized coupling constant. When $\lambda'\to\infty$, both saddle points $v_\pm$ will give comparable contributions and both should be included.

The asymptotics of the other terms (59) and (60) can be computed by similar considerations. These functions are defined as double integrals. The first one is taken from 0 to ∞ and the second from $-\infty$ to ∞. To compute their asymptotic behavior for large s, the latter integral should be deformed into the complex plane as was done above and in the former integral one has to take into account only the lowest-order terms according to expansion (A26).

Let us consider the first term in Eq. (59). We need to know the limiting behavior of the integrand when $\alpha_1\to 0$ and $\alpha_2+\alpha_1=iv$ (we prefer to use this deformation instead of the usual one, $\alpha_2=iv$, to simplify the formulas below). From Eqs. (A17), (A26), and (A30) it follows that for real α,

$$\tilde{J}_1(\alpha_1, iv-\alpha_1) \overset{\alpha_1\simeq 0}{\rightarrow} I(v)+e^v\left(\frac{\pi}{2}-i(2\gamma+\ln v-1+\ln\alpha_1)\right)\alpha_1, \quad (70)$$

with $I(v)$ defined by Eq. (62). From Eq. (A22) in this limit $R(\alpha)\simeq\pi\alpha_1 e^v$. The dominant contribution in $V_{\phi_1,\phi_1}(\alpha)$ comes from the second term in Eq. (44) and one gets $V_{\phi_1,\phi_1}(\alpha)\simeq -i\langle e^{vr}\rangle^2/(\alpha_1 v)$. Combining all terms together and changing the variable $\alpha_1\to\alpha/(s\langle re^{rv}\rangle)$ we find that at large s

$$A(s)=2\pi i\int_0^\infty d\alpha\int_{-i\infty}^{+i\infty}\frac{dv}{v}(\langle e^{rv}\rangle)^2 e^{-s[\langle I(vr)\rangle - v/\lambda']}$$
$$\times e^{-\pi\alpha/2}\sin\{\alpha[\ln\alpha-\ln s+g(v)]\}+(\lambda'\to-\lambda'), \quad (71)$$

where

$$g(v)=\ln v+2\gamma-1+2\frac{\langle re^{rv}\ln r\rangle}{\langle re^{rv}\rangle}-\ln\langle re^{rv}\rangle. \quad (72)$$

The integral over v is an analog of Eq. (64) and can be computed exactly as above:

$$A(s)=-(2\pi)^{3/2}\sum_{i=\pm}\frac{(\langle e^{rv_i}\rangle)^2}{\sqrt{\langle re^{rv_i}\rangle s v_i}}$$
$$\times f[\ln s-g(v_i)]e^{-s(\langle e^{rv_i}\rangle-1)}, \quad (73)$$

where the function $f(y)$ is given by the integral

$$f(y)=\int_0^\infty e^{-\pi\alpha/2}\sin[\alpha(\ln\alpha-y)]d\alpha. \quad (74)$$

One can check that the contribution (60) when $s\to\infty$ is smaller by a factor $1/s$ with respect to Eqs. (68) and (73) and can be neglected.

Finally, we obtain that the nearest-neighbor distribution, $P(s)$, in the limit of large s has the following asymptotics:

$$P(s)=\frac{(\langle e^{rv_{\mathrm{sp}}}\rangle)^2}{\sqrt{2\pi\langle re^{rv_{\mathrm{sp}}}\rangle v_{\mathrm{sp}}}}$$
$$\times\frac{e^{-s\langle e^{rv_{\mathrm{sp}}}\rangle}}{\sqrt{s}}\{1-f[\ln s-g(v_{\mathrm{sp}})]\}. \quad (75)$$

The saddle-point value, v_{sp}, depends on the renormalized coupling constant by Eq. (69),

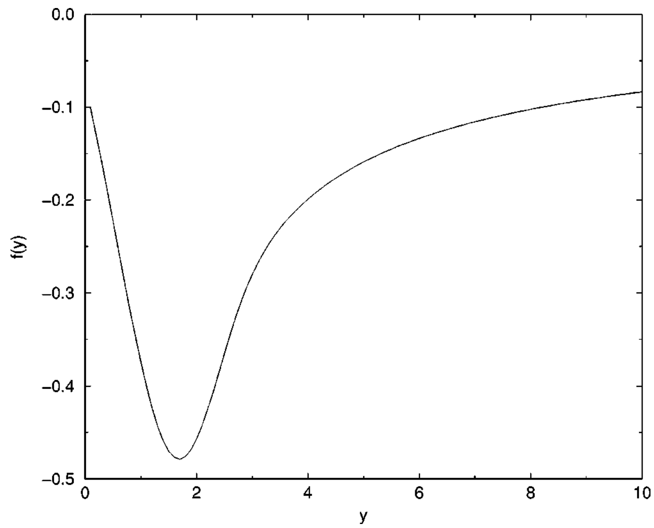

FIG. 2. Plot of the function $f(y)$ defined in Eq. (74).

$$-\langle r\,\mathrm{Ei}(r v_{\mathrm{sp}})\rangle=\frac{1}{|\lambda'|}. \tag{76}$$

When λ is very large, the contribution of the second saddle point with a reversed sign of the right-hand side of this equation should be added.

In Fig. 2, the plot of the function $f(y)$ defined in Eq. (74) is presented. When $y\to\infty$, this function goes to zero as $-1/y$. Therefore, the true asymptotics of $P(s)$ is given by the first term in Eq. (75),

$$P(s)=\frac{(\langle e^{r v_{\mathrm{sp}}}\rangle)^2}{\sqrt{2\pi\langle r e^{r v_{\mathrm{sp}}}\rangle v_{\mathrm{sp}}}}\frac{e^{-s\langle e^{r v_{\mathrm{sp}}}\rangle}}{\sqrt{s}}. \tag{77}$$

But because in Eq. (75) the argument of the function $f(y)$ up to the constant (72) is $\ln s$, this decrease is quite slow, and at numerically accessible values of s of the order of 10 (i.e., y of the order of 3–4) as is evident from Fig. 2 this function gives a noticeable contribution.

For the billiard with periodic boundary conditions, the residues in Eq. (7) all equal 1, and all mean values are reduced to the corresponding function, i.e., for any function f the quantity $\langle f(rx)\rangle$ becomes $f(x)$.

In this case, the nearest-neighbor distribution has the following asymptotics:

$$P(s)=\sqrt{\frac{e^{3v_{\mathrm{sp}}}}{2\pi v_{\mathrm{sp}}}}\frac{e^{-s e^{v_{\mathrm{sp}}}}}{\sqrt{s}}[1-f(\ln s-g(v_{\mathrm{sp}}))]. \tag{78}$$

The value of v_{sp} is determined by the equation

$$\mathrm{Ei}(v_{\mathrm{sp}})=-\frac{1}{|\lambda'|} \tag{79}$$

and

$$g(v_{\mathrm{sp}})=\ln v_{\mathrm{sp}}-v_{\mathrm{sp}}+2\gamma-1. \tag{80}$$

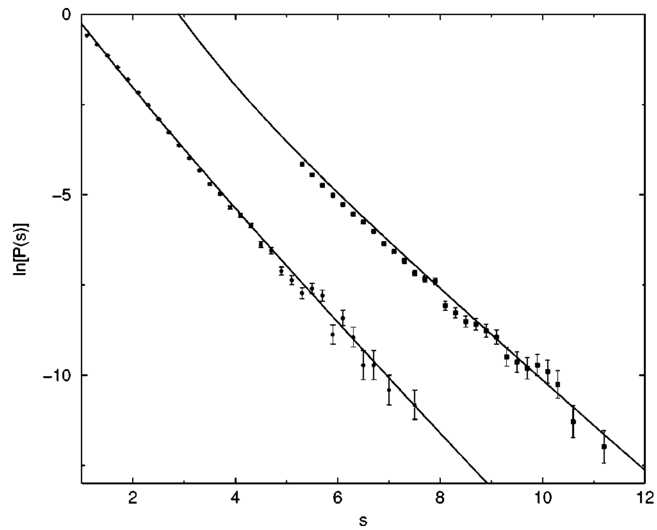

FIG. 3. The nearest-neighbor distribution in the periodic case. Squares and circles correspond, respectively, to $\lambda'=1$ and $\lambda'=100$. Solid lines: theoretical predictions (78). For clarity, the upper curves are shifted to the right by two units.

In Fig. 3, we present a comparison between numerical computations and the theoretical prediction (78) for two values of λ. The logarithm of the nearest-neighbor distribution is plotted as a function of s. The upper curve (squares) corresponds to 10^6 levels with $\lambda'=1$ and the lower one (circles) to 5×10^5 levels with $\lambda'=100$. For clarity, the curve corresponding to $\lambda'=1$ has been shifted on the right by $s\to s+2$. The solid lines represent theoretical predictions (78) for these values of the coupling constant. For $\lambda'=100$, two saddle points with a different sign of the right-hand side of Eq. (79) have been taken into account, which roughly doubles the result (78). These results confirm very well the theoretical asymptotics of the nearest-neighbor distribution (78).

In the case of a rectangular billiard of size $a\times b$ with Dirichlet boundary conditions, with a pointlike scatterer such that the ratios of its positions (x_0,y_0) to the corresponding sides are noncommensurable irrational numbers, the residues, r_n, can be considered as random variables of the form given by Eq. (12) and the mean value of a given function $f,\langle f(r)\rangle$, should be computed as follows:

$$\langle f(r)\rangle=\frac{4}{\pi^2}\int_0^{\pi/2}d\phi_1\int_0^{\pi/2}d\phi_2\quad f(4\sin^2\phi_1\sin^2\phi_2). \tag{81}$$

In the case where x_0/a and y_0/b are rational numbers (13), the mean value $\langle f(r)\rangle$ takes the form (see [13])

$$\langle f(r)\rangle=\frac{1}{q_1q_2}\sum_{k_1=0}^{q_1-1}\sum_{k_2=0}^{q_2-1}f\left(4\sin^2\frac{\pi k_1}{q_1}\sin^2\frac{\pi k_2}{q_2}\right). \tag{82}$$

The cases $k_1=0$ and $k_2=0$ correspond to unperturbed subsequence of levels (for Dirichlet boundary conditions) and one has the freedom to include them in the level density (17) or consider them separately. In the latter case, the terms with

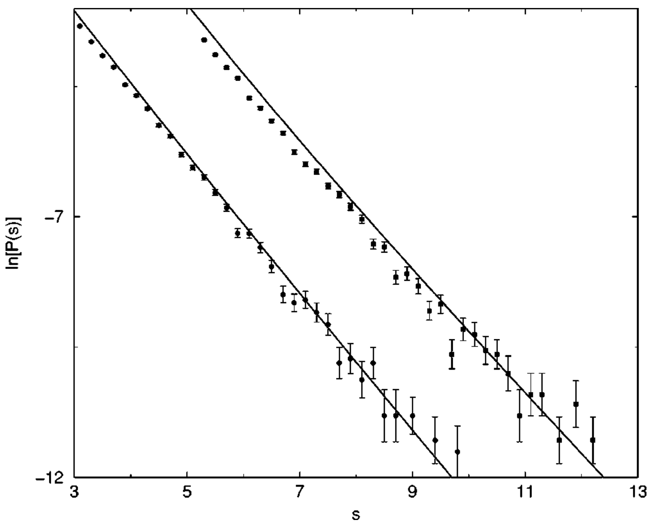

FIG. 4. The nearest-neighbor distribution for a billiard with Dirichlet boundary conditions. Squares and circles correspond, respectively, to $\lambda'=1$ and $\lambda'=10$. Solid lines: theoretical asymptotics (78). Upper curves are shifted to the right by two units.

$k_i=0$ should be omitted and $1/(q_1q_2)$ in front of the sum should be substituted by $1/[(q_1-1)(q_2-1)]$. The generalizations of $\langle f(r)\rangle$ for the case in which only one ratio x_0/a or y_0/b is an irrational number and the other one is a rational number, or both ratios are irrational but commensurable numbers, are straightforward.

With such a definition of the mean value, the asymptotics of the nearest-neighbor distribution is given by Eq. (75).

As in the periodic case, the quantity $-\ln P(s)$ is expected to be nearly linear with the slope $\langle e^{rv_{\rm sp}}\rangle$, where $v_{\rm sp}$ is the solution of Eq. (76).

Figure 4 shows a comparison between the numerically computed nearest-neighbor distribution for a billiard with Dirichlet boundary conditions and the expected asymptotic behavior (75) (solid line) for two values of the renormalized coupling constant, $\lambda'=1$ and $\lambda'=10$ ($x_0/a, y_0/b$ are incommensurable irrational numbers). To better understand the asymptotics of the nearest-neighbor distribution, we present in Fig. 5 the functions which determine the exponential decrease of $P(s)$. Different curves in this figure correspond to the following functions: $-\mathrm{Ei}(x)$ (thick solid line), $\exp x$ (thin solid line), $-\langle r\mathrm{Ei}(rx)\rangle$ (thick dashed line), and $\langle \exp x\rangle$ (thin dashed line).

For periodic boundary conditions, the intersection of the horizontal line having the ordinate $1/\lambda'$ with the graph of $-\mathrm{Ei}(x)$ gives the value of $v_{\rm sp}$. The point of intersection of the vertical line going through $v_{\rm sp}$ with the graph of e^x determines the exponent in Eq. (78). For Dirichlet boundary conditions, one should use the same procedure but with the functions $-\langle r\mathrm{Ei}(rx)\rangle$ and $\langle e^{rx}\rangle$.

IV. THE *n*TH NEAREST-NEIGHBOR SPACING DISTRIBUTION

In the previous sections we compute the nearest-neighbor distribution, $P(s)$, for a rectangular billiard with a small-size scattering center inside, i.e., the probability that two levels are separated by a distance s with no levels in between. In this section, we generalize the formalism to compute the nth nearest-neighbor distribution, $P_n(s)$, which is defined as the probability that two levels at distance s are separated by n levels, for $n\geqslant 1$.

Our starting point is the expression (41) which is valid for any sequence σ_k of 0 and 1. To obtain the nth nearest-neighbor distribution, one should sum over all sequences of length N with exactly $n+1$ zeros. Performing the same steps as in Sec. II B and taking into account that when $N\to\infty$ we have $C_N^n\to N^n/n!$, one obtains

$$P_n(s)=e^{-s}\int_{-\infty}^{\infty}\frac{d\alpha_1 d\alpha_2}{(2\pi)^2}\Bigg(\frac{s^{n+1}}{(n+1)!}[1-\langle\tilde{J}_0(\alpha r)\rangle]^{n+1}V_{\phi_1,\phi_1}(\alpha)+\frac{s^n}{n!}[1-\langle\tilde{J}_0(\alpha r)\rangle]^n[V_{\phi_0,\phi_1}(\alpha)+V_{\phi_1,\phi_0}(\alpha)]$$
$$+\frac{s^{n-1}}{(n-1)!}[1-\langle\tilde{J}_0(\alpha r)\rangle]^{n-1}V_{\phi_0,\phi_0}(\alpha)\Bigg)e^{-s[\langle\tilde{J}_1(\alpha r)\rangle+i(\alpha_1+\alpha_2)/\lambda']},\qquad(83)$$

with all functions defined as above.

As a consistency check, one can verify that the sum over all n coincides with the exact expression of the two-point correlation function derived in [13],

$$R_2(s)=\sum_{n=0}^{\infty}P_n(s).\qquad(84)$$

Similarly to Sec. II C, the different terms in Eq. (83) can be classified according to their analytical properties. Three groups of terms appear. The first group has terms which have the same analytical properties as the function $\tilde{J}_1(\alpha)$ in the exponent. Exactly as was done in Sec. II C, one can argue that their contribution is zero because one can freely move the integration contour to infinity. The second group consists of terms which are singular on one variable but have "good" analytical properties on the other variable of integration. The large s asymptotics of such terms can be calculated as in Sec. III by computing the leading terms over the former variable and shifting the contour of integration over the latter variable into the complex plane until it reaches the saddle point. The asymptotics of these terms will be proportional to exp

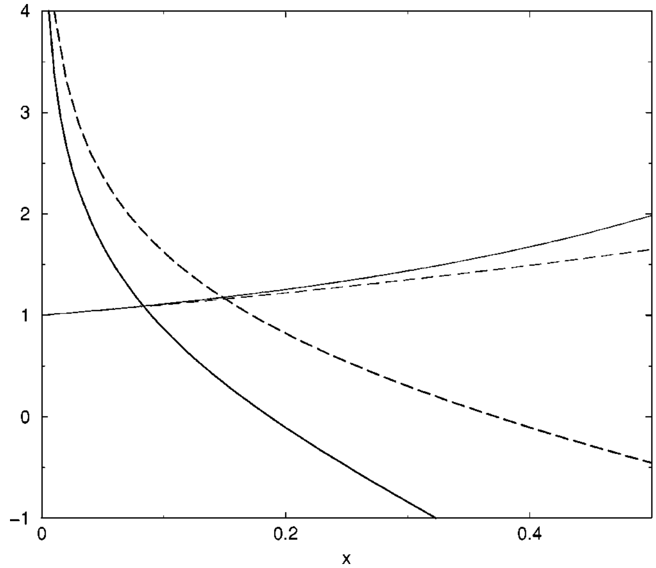

FIG. 5. Functions $-\mathrm{Ei}(x)$ (thick solid line), $-\langle r\mathrm{Ei}(rx)\rangle$ (thick dashed line), e^x (thin solid line), and $\langle e^{rx}\rangle$ (thin dashed line).

$[-se^{v_{\mathrm{sp}}}]$ as for the nearest-neighbor distribution. Finally, the third group [which does not exist for $P(s)$] includes terms which are singular [i.e., have analytical properties different from that of $\tilde{J}_1(\alpha)$] for both variables of integration. In this case, no deformation of the integration contour is possible, the region of small α_1 and α_2 will be important, and the asymptotic result will be proportional to $\exp(-s)$. As $v_{\mathrm{sp}}>0$, it is the last group of terms which will dominate the asymptotics of $P_n(s)$ when $s\to\infty$.

From formula (A26) of the Appendix it follows that, when both variables α_1 and α_2 are small, the functions V_{ϕ_i,ϕ_j} will be equivalent to their singular parts,

$$V_{\phi_1,\phi_1}(\alpha)\simeq\frac{1}{\alpha_1\alpha_2},\quad V_{\phi_1,\phi_0}(\alpha)\simeq-\frac{2\pi i}{\alpha_1}\delta(\alpha_2),$$

$$V_{\phi_1,\phi_0}(\alpha)\simeq\frac{2\pi i}{\alpha_2}\delta(\alpha_1),\quad V_{\phi_0,\phi_0}(\alpha)\simeq(2\pi)^2\delta(\alpha_1)\delta(\alpha_2). \tag{85}$$

The singular terms in $[1-\langle\tilde{J}_0(r\alpha)\rangle]^n$ are given by the small-α behavior in Eq. (A25). Keeping only the terms with a singularity in $\{1+\langle\tilde{J}_1(r\alpha)\rangle-[\langle\tilde{J}_0(r\alpha)\rangle+\langle\tilde{J}_1(r\alpha)\rangle]\}^n$, we get

$$[1-\langle\tilde{J}_0(r\alpha)\rangle]^n=1-n\pi(|\alpha_1|+|\alpha_2|)+n(n-1)\pi^2|\alpha_1||\alpha_2|. \tag{86}$$

(We recall that the terms coming from $\tilde{J}_1$ vanish.) The first term in this expression is the dominant regular contribution, the second one is the dominant contribution singular in one variable, and the third term is the dominant contribution singular in both variables.

Combining all the above expressions together and using Eq. (A24), we obtain

$$P_n(s)=\frac{s^{n-1}}{(n-1)!}e^{-s}\int_{-\infty}^{\infty}\frac{d\alpha_1 d\alpha_2}{(2\pi)^2}[\pi^2s^2\mathrm{sgn}(\alpha_1)\mathrm{sgn}(\alpha_2)+2\pi^2is\,\mathrm{sgn}(\alpha_1)\delta(\alpha_2)-2\pi^2is\,\mathrm{sgn}(\alpha_2)\delta(\alpha_1)+(2\pi)^2\delta(\alpha_1)\delta(\alpha_2)]\exp-s\left(\frac{\pi}{2}(|\alpha_1|+|\alpha_2|)-i\alpha_1(\ln|\alpha_1|+g_-)+i\alpha_2(\ln|\alpha_2|+g_+)\right), \tag{87}$$

where

$$g_\pm=\langle r\ln r\rangle+\gamma-1\pm\frac{1}{\lambda'}. \tag{88}$$

After simple calculations, we obtain the large-s asymptotics of the nth nearest-neighbor distribution

$$P_n(s)=\frac{s^{n-1}}{(n-1)!}e^{-s}[1-f(\ln s-g_+)][1-f(\ln s-g_-)], \tag{89}$$

where the function $f(y)$ is defined by Eq. (74) (see also Fig. 2).

The only difference between periodic and Dirichlet boundary conditions is in the constant $g_\pm$ (88) where the term $\langle r\ln r\rangle=2(1-\ln 2)$ is added for the latter.

As above, when $s\to\infty$ the function $f(\ln s-g_\pm)$ goes to zero and the true asymptotics of the nth nearest-neighbor distribution with $n\geqslant1$ for all boundary conditions is

$$P_n(s)=\frac{s^{n-1}}{(n-1)!}e^{-s}, \tag{90}$$

i.e., it coincides with the $(n-1)$th nearest-neighbor distribution for the Poisson distribution. A simple physical explanation of this result is the following.

We are interested in the solutions of Eq. (7) when unperturbed levels, e_j, are independent random variables. Among all configurations of e_j there are cases where two unperturbed levels e_1 and e_2 are very close to each other. In such a case, Eq. (7) reduces to two terms

$$\frac{r_1}{E-e_1}+\frac{r_2}{E-e_2}=0, \tag{91}$$

which has a simple solution

$$E=\frac{e_1r_2+e_2r_1}{r_1+r_2}. \tag{92}$$

As we assume that the difference e_1-e_2 is very small, the value of E will also be very close to both unperturbed levels, e_1 and e_2. Equation (92) can be reversed, and having one unperturbed level, say e_1, and a new level, E, very close to it, one can always find the position of another unperturbed level, e_2, to fulfill Eq. (7) in that approximation. We shall call two very close unperturbed levels with a new level inside a dipole configuration. Now let us consider the probability that two unperturbed levels e_1 and e_2 are at the distance s with $n-1$ unperturbed levels inside this interval. As unperturbed levels are independent, this probability is given by Eq. (90).

We represent in Fig. 6 a possible configuration for two unperturbed levels (short thin vertical lines) separated by a large distance $s=e_1-e_2$ with $n-1$ levels between them. For any such configuration, there exists a configuration with two new energy levels at E_2 and E_1, very close to e_2 and e_1 respectively. This is true because, as we have pointed out, it is possible to construct two unperturbed energy levels e_2' and e_1' (indicated by dashed lines in Fig. 6) such that two pairs $(e_2',e_2),(e_1',e_1)$ form the dipoles. For that configuration it is clear that E_2 and E_1 are two perturbed levels with n perturbed levels in between. When $s\to\infty$, it is physically clear that the other levels will not influence these dipole configurations, which explains Eq. (90).

It is clear that this reasoning cannot be applied to the nearest-neighbor distribution (as it requires at least two unperturbed levels inside the interval s) and the asymptotics of $P(s)$ given by Eq. (77) is quite different from Eq. (90).

To check the asymptotic formula (90), we compute numerically the nth nearest-neighbor distributions until $n=9$ for a rectangular billiard with size $4\times\pi$ with periodic boundary conditions and for different coupling constants. First, we find the best fit of the integrated nth nearest-neighbor distribution $N_n(s)=\int_0^s P_n(t)dt$ in the form $a\exp(bs)s^c$. In Fig. 7, we plot values of b and c obtained by this fit. The lower curve (dots) shows the values of the constant b, which, as expected, is the same for all values of n and is equal with a good precision to -1. The upper curve (squares) shows the exponent c, which according to Eq. (89) is expected to be $n-1$. This is indeed the case for the higher values of n. The small deviations from this expected value for the lowest n come from the fact that the function f has to be taken into account since for large s, $f(\ln s-g_{\pm})$ behaves like $1/\ln s$. To illustrate the accuracy of Eq. (89) we present in Fig. 8 the results of numerical computations for $P_2(s)$ and $P_8(s)$ for a billiard with periodic boundary conditions and renormalized coupling constant, $\lambda'=1$. Error bars in this figure indicate statistical errors. It is clear that the asymptotic formula (89) describes well the large s behavior of $P_n(s)$.

The same checks have been performed for billiards with Dirichlet boundary conditions. The results are presented in Fig. 9 and Fig. 10. Again the theoretical asymptotics (89) is in a good agreement with numerical results.

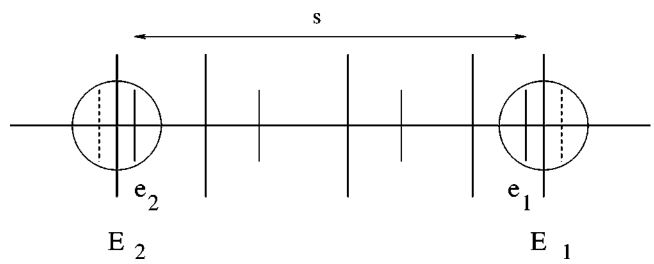

FIG. 6. Schematic representation of the dominant contribution to the nth nearest-neighbor distribution. Thin vertical lines are unperturbed energy levels. Thick lines represent new energy levels. Two vertical dashed lines indicate two unperturbed energy levels which are added to construct encircled dipole configurations.

V. CONCLUSION

The starting point of our investigation is Eq. (7),

$$\lambda\sum_{j=1}^{N}\frac{r_j}{E-e_j}=1. \tag{93}$$

We assume that (i) all e_j are independent random variables, (ii) the residues r_j are real positive, and we compute the nth nearest-neighbor distribution $P_n(s)$ of the solutions, E, in the limit $N\to\infty$. The exact formulas are quite cumbersome and we dwell on the asymptotic behavior of $P_n(s)$ at large s. Our main results are the following.

The asymptotics of the nearest-neighbor distribution, $P(s)$, is given by Eq. (77) and has the form

$$P(s)=\frac{(\langle e^{rv_{\rm sp}}\rangle)^2}{\sqrt{2\pi\langle re^{rv_{\rm sp}}\rangle v_{\rm sp}}}\frac{e^{-s\langle e^{rv_{\rm sp}}\rangle}}{\sqrt{s}}. \tag{94}$$

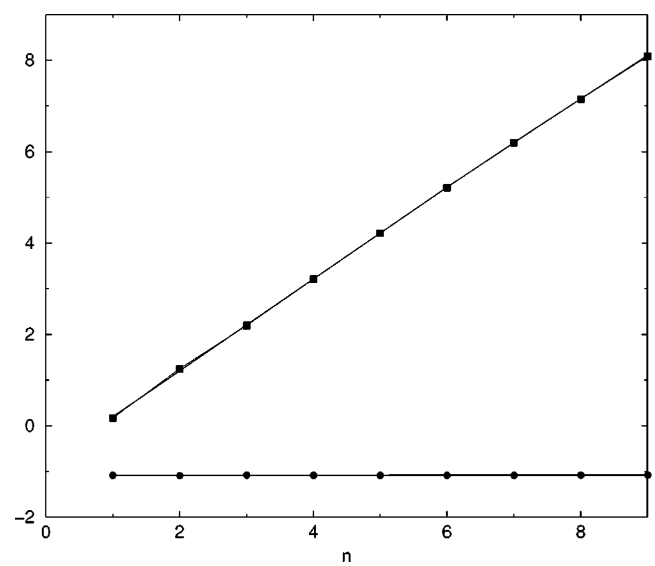

FIG. 7. Values of b (dots) and c (squares) in a fit of $N_n(s)$ for periodic boundary conditions under the form $a\exp(bs)s^c$.

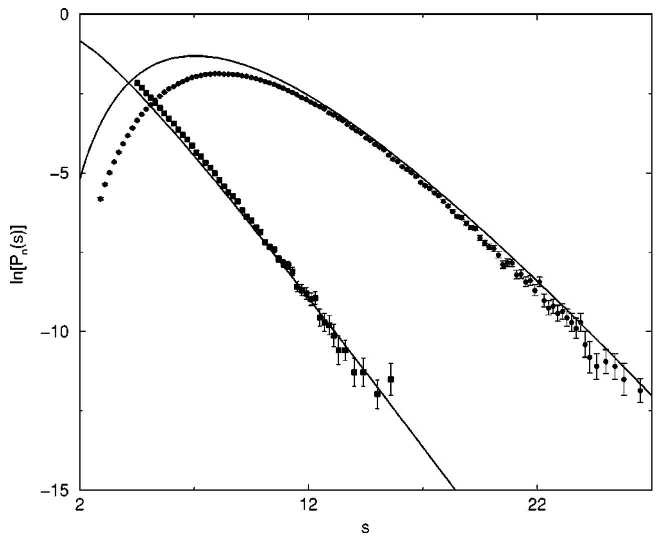

FIG. 8. $P_2(s)$ (the left curve) and $P_8(s)$ (the right curve) for a billiard with periodic boundary conditions.

Here v_{sp} is determined by the equation

$$-\langle r\mathrm{Ei}(rv_{sp})\rangle = \frac{1}{|\lambda'|}, \tag{95}$$

where Ei(x) is the usual exponential integral (63) and λ' is the renormalized coupling constant (48). The notation $\langle f(r)\rangle$ indicates the mean value over all residues. For periodic boundary conditions $\langle f(r)\rangle = f(1)$. For Dirichlet conditions $\langle f(r)\rangle$ depends on the ratios of the coordinates of the scatterer to the corresponding sides. When these ratios are noncommensurable irrational numbers, $\langle f(r)\rangle$ is defined in Eq. (81). When they are rational numbers, $\langle f(r)\rangle$ should be computed as in Eq. (82).

The nth nearest-neighbor distribution with $n \geqslant 1$ when $s \to \infty$ has the following asymptotics:

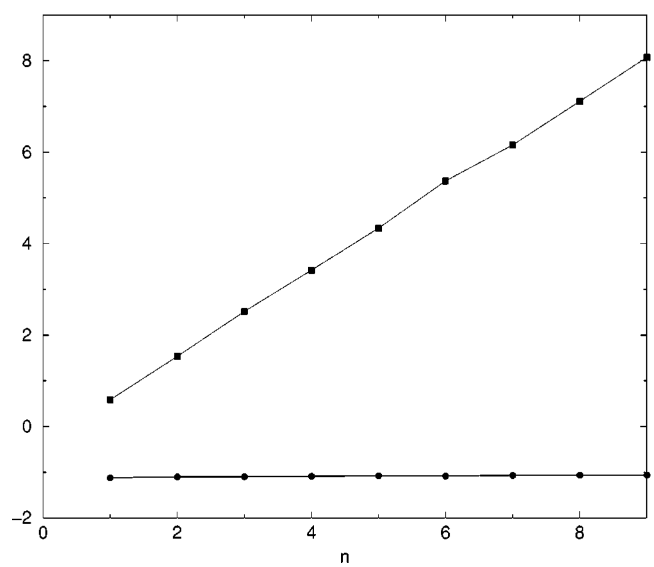

FIG. 9. Values of b (dots) and c (squares) in a fit of $N_n(s)$ for Dirichlet boundary conditions under the form $a\,\exp(bs)s^c$.

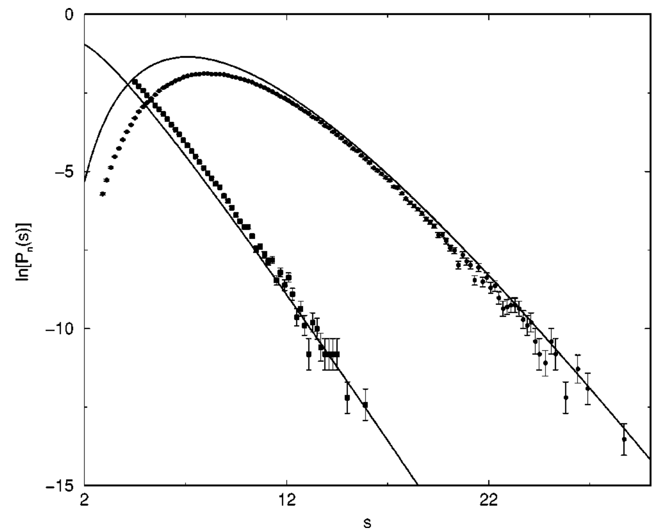

FIG. 10. $P_2(s)$ (the left curve) and $P_8(s)$ (the right curve) for a billiard with Dirichlet boundary condition.

$$P_n(s) = \frac{s^{n-1}}{(n-1)!}e^{-s}, \tag{96}$$

which depends neither on the residues nor on the boundary conditions. For finite values of s there are slowly decreasing corrections to these formulas indicated in Eqs. (75) and (89) which are important for accurate comparison with results of numerical calculations.

The above results together with the results of Ref. [13] prove that spectral statistics of generic rectangular billiards with a small-size scattering center inside is of special (intermediate) type characterized by two important properties: (i) level repulsion at small s and (ii) exponential decrease of the nearest-neighbor distribution at large s. To the best of our knowledge, this is the first example of a dynamical system where the intermediate character of the spectral statistics can be proved rigorously.

ACKNOWLEDGMENTS

Laboratoire de Physique Théorique et Modèles Statistiques is Unité Mixte de Recherche de l'Université Paris XI et du CNRS (UMR 8626).

APPENDIX

The purpose of this Appendix is the computation of two main integrals,

$$\tilde{J}_1(\alpha_1,\alpha_2) = \left(\int_{-\infty}^{0} + \int_{1}^{\infty}\right)\left[1-\exp\left(i\frac{\alpha_1}{1-e} - i\frac{\alpha_2}{e}\right)\right]de \tag{A1}$$

and

$$\tilde{J}_0(\alpha_1,\alpha_2) = \int_0^1\left[1-\exp\left(i\frac{\alpha_1}{1-e} - i\frac{\alpha_2}{e}\right)\right]de. \tag{A2}$$

As in [13], we first find the difference of the derivatives over α_1 and α_2,

$$(\partial_1-\partial_2)\tilde{J}_1(\alpha_1,\alpha_2) = -i\left(\int_{-\infty}^{0}+\int_{1}^{\infty}\right)\frac{de}{e(1-e)}\exp\left(i\frac{\alpha_1}{1-e}-i\frac{\alpha_2}{e}\right), \tag{A3}$$

where ∂_i denotes the partial derivative with respect to the α_i. Changing the variable $e=t/(1+t)$, one gets

$$(\partial_1-\partial_2)\tilde{J}_1(\alpha_1,\alpha_2)=e^{i(\alpha_1-\alpha_2)}\phi_1(\alpha_1,\alpha_2), \tag{A4}$$

where

$$\phi_1(\alpha_1,\alpha_2)=i\int_0^\infty\frac{dt}{t}\exp\left(-i\alpha_1 t+i\frac{\alpha_2}{t}\right). \tag{A5}$$

The last integral is well defined for complex α when $\mathrm{Im}(\alpha_1)<0$ and $\mathrm{Im}(\alpha_2)>0$. In this domain (see [23]),

$$\phi_1(\alpha_1,\alpha_2)=2iK_0(2\sqrt{\alpha_1\alpha_2}), \tag{A6}$$

where $K_0(x)$ is the modified Bessel function of the third kind. At real α, the limiting function is discontinuous and depends on the sign of α,

$$\phi_1(\alpha_1,\alpha_2) = \begin{cases} -\pi H_0^{(1)}(2\sqrt{-\alpha_1\alpha_2}) & \text{when} \quad \alpha_1<0,\ \alpha_2>0 \\ 2iK_0(2\sqrt{\alpha_1\alpha_2}) & \text{when} \quad \alpha_1>0,\ \alpha_2>0 \\ \pi H_0^{(2)}(2\sqrt{-\alpha_1\alpha_2}) & \text{when} \quad \alpha_1>0,\ \alpha_2<0 \\ 2iK_0(2\sqrt{\alpha_1\alpha_2}) & \text{when} \quad \alpha_1<0,\ \alpha_2<0. \end{cases} \tag{A7}$$

The function $\tilde{J}_0(\alpha)$ obeys the similar equation

$$(\partial_1-\partial_2)\tilde{J}_0(\alpha_1,\alpha_2)=e^{i(\alpha_1-\alpha_2)}\phi_0(\alpha_1,\alpha_2), \tag{A8}$$

where

$$\phi_0(\alpha_1,\alpha_2)=-i\int_0^\infty\frac{dt}{t}\exp\left(i\alpha_1 t-i\frac{\alpha_2}{t}\right) = -2iK_0(2\sqrt{\alpha_1\alpha_2}), \tag{A9}$$

which is defined in the region $\mathrm{Im}(\alpha_1)>0$ and $\mathrm{Im}(\alpha_2)<0$. At real α, $\phi_0(\alpha)=\phi_1^*(\alpha)$ or explicitly

$$\phi_0(\alpha_1,\alpha_2) = \begin{cases} -\pi H_0^{(2)}(2\sqrt{-\alpha_1\alpha_2}) & \text{when} \quad \alpha_1<0,\ \alpha_2>0 \\ -2iK_0(2\sqrt{\alpha_1\alpha_2}) & \text{when} \quad \alpha_1>0,\ \alpha_2>0 \\ \pi H_0^{(1)}(2\sqrt{-\alpha_1\alpha_2}) & \text{when} \quad \alpha_1>0,\ \alpha_2<0 \\ -2iK_0(2\sqrt{\alpha_1\alpha_2}) & \text{when} \quad \alpha_1<0,\ \alpha_2<0. \end{cases} \tag{A10}$$

We note also the expression for the sum of $\phi_\sigma(\alpha)$,

$$\phi_1(\alpha_1,\alpha_2)+\phi_0(\alpha_1,\alpha_2) = \pi[\mathrm{sgn}(\alpha_1)-\mathrm{sgn}(\alpha_2)]J_0(2\sqrt{-\alpha_1\alpha_2}), \tag{A11}$$

where $\mathrm{sgn}(x)$ denotes the sign of x.

The knowledge of $\phi_\sigma(\alpha)$ permits us to write down a linear partial derivative equation for $J_\sigma(\alpha)$,

$$(\partial_1-\partial_2)\tilde{J}_\sigma(\alpha_1,\alpha_2)=Z_\sigma(\alpha_1,\alpha_2), \tag{A12}$$

where

$$Z_\sigma(\alpha_1,\alpha_2)=e^{i(\alpha_1-\alpha_2)}\phi_\sigma(\alpha_1,\alpha_2). \tag{A13}$$

The general solution of this equation has the form

$$\tilde{J}_\sigma(\alpha_1,\alpha_2)=\tilde{J}_\sigma(0,\alpha_1+\alpha_2) + \int_0^{\alpha_1}Z_\sigma(t,\alpha_1+\alpha_2-t)dt. \tag{A14}$$

The initial values $\tilde{J}_\sigma(0,\alpha)$ can be computed directly from the definitions (A1) and (A2). By changing the variable e to $t=-1/e$, one gets

$$\tilde{J}_1(0,\alpha)=\left(\int_{-\infty}^{0}+\int_{1}^{\infty}\right)(1-e^{-i\alpha/e})de = ⨍_{-1}^{\infty}\frac{dt}{t^2}(1-e^{i\alpha t}), \tag{A15}$$

where ⨍ is the principal value of the integral. Similarly

$$\tilde{J}_0(0,\alpha)=\int_0^1(1-e^{-i\alpha/e})de=\int_1^\infty\frac{dt}{t^2}(1-e^{-i\alpha t}). \tag{A16}$$

The final expressions for $\tilde{J}_\sigma(\alpha)$ are the following:

$$\tilde{J}_1(\alpha_1,\alpha_2)=⨍_{-1}^{\infty}\frac{dt}{t^2}(1-e^{i(\alpha_1+\alpha_2)t}) + \int_0^{\alpha_1}e^{i(2t-\alpha_1-\alpha_2)}\phi_1(t,\alpha_1+\alpha_2-t)dt \tag{A17}$$

and

$$\tilde{J}_0(\alpha_1,\alpha_2)=\int_1^\infty\frac{dt}{t^2}(1-e^{-i(\alpha_1+\alpha_2)t}) + \int_0^{\alpha_1}e^{i(2t-\alpha_1-\alpha_2)}\phi_0(t,\alpha_1+\alpha_2-t)dt. \tag{A18}$$

According to Eqs. (A2) and (A1), the functions $\tilde{J}_0(\alpha)$ and $\tilde{J}_1(\alpha)$ considered as functions of complex α_1 and α_2 are analytical functions in different regions: $\mathrm{Im}(\alpha_1)>0$ and $\mathrm{Im}(\alpha_2)<0$ for the former and $\mathrm{Im}(\alpha_1)<0$ and $\mathrm{Im}(\alpha_2)>0$ for the latter. They can be continued to complex planes with the cuts represented in Figs. 1(a) and 1(b) for $\tilde{J}_1$ and in Figs. 1(c) and 1(d) for $\tilde{J}_0$. At real values of α_1 and α_2 they have a discontinuity along the axis $\alpha_1=0$ and $\alpha_2=0$.

The sum $\tilde{J}_0(\alpha)+\tilde{J}_1(\alpha)$ obeys an equation similar to Eq. (A4), where instead of function $\phi_1(\alpha)$ one substitutes the sum (A11),

$$(\partial_1-\partial_2)[\tilde{J}_1(\alpha_1,\alpha_2)+\tilde{J}_0(\alpha_1,\alpha_2)] \\ =e^{i(\alpha_1-\alpha_2)}Z(\alpha_1,\alpha_2), \quad \text{(A19)}$$

where

$$Z(\alpha_1,\alpha_2)=\pi[\mathrm{sgn}(\alpha_1)-\mathrm{sgn}(\alpha_2)]J_0(2\sqrt{-\alpha_1\alpha_2}). \quad \text{(A20)}$$

The solution of these equations can be done exactly as above and it can be represented as a sum of two discontinuous functions,

$$\tilde{J}_0(\alpha_1,\alpha_2)+\tilde{J}_1(\alpha_1,\alpha_2) \\ =\mathrm{sgn}(\alpha_1)R(\alpha_1,\alpha_2)+\mathrm{sgn}(\alpha_2)R^*(\alpha_2,\alpha_1), \quad \text{(A21)}$$

where

$$R(\alpha_1,\alpha_2)=\pi\int_0^{\alpha_1}J_0[2\sqrt{-t(\alpha_1+\alpha_2-t)}] \\ \times e^{i(2t-\alpha_1-\alpha_2)}dt. \quad \text{(A22)}$$

One can check that this expression coincides with Eq. (A24) of [13].

The following useful symmetry properties can be checked directly from the definitions (A1) and (A2):

$$\tilde{J}_\sigma(\alpha_2,\alpha_1)=\tilde{J}_\sigma(-\alpha_1,-\alpha_2)=\tilde{J}_\sigma^*(\alpha_1,\alpha_2),$$

$$\phi_\sigma(\alpha_2,\alpha_1)=\phi_\sigma(-\alpha_1,-\alpha_2)=-\phi_\sigma^*(\alpha_1,\alpha_2),$$

$$R(-\alpha_1,-\alpha_2)=-R^*(\alpha_1,\alpha_2). \quad \text{(A23)}$$

For further references we present the behavior of $\tilde{J}_\sigma(\alpha)$ and $\phi_\sigma(\alpha)$ at small real α,

$$\tilde{J}_1(\alpha_1,\alpha_2)=\frac{\pi}{2}(|\alpha_1|+|\alpha_2|)+i\alpha_1(1-\gamma-\ln|\alpha_1|) \\ -i\alpha_2(1-\gamma-\ln|\alpha_2|), \quad \text{(A24)}$$

$$\tilde{J}_0(\alpha_1,\alpha_2)=\frac{\pi}{2}(|\alpha_1|+|\alpha_2|)-i\alpha_1(1-\gamma-\ln|\alpha_1|) \\ +i\alpha_2(1-\gamma-\ln|\alpha_2|), \quad \text{(A25)}$$

and

$$\phi_1(\alpha_1,\alpha_2)=\frac{\pi}{2}[\mathrm{sgn}(\alpha_1)-\mathrm{sgn}(\alpha_2)] \\ -i(2\gamma+\ln|\alpha_1|+\ln|\alpha_2|), \quad \text{(A26)}$$

$$\phi_0(\alpha_1,\alpha_2)=\frac{\pi}{2}[\mathrm{sgn}(\alpha_1)-\mathrm{sgn}(\alpha_2)] \\ +i(2\gamma+\ln|\alpha_1|+\ln|\alpha_2|), \quad \text{(A27)}$$

where γ is the Euler constant.

Due to the above-mentioned analytical properties, these expressions (though they have apparent discontinuities) can be rewritten as the following analytical functions:

$$\tilde{J}_1(\alpha_1,\alpha_2)=i\alpha_1[1-\gamma-\ln(i\alpha_1)] \\ -i\alpha_2[1-\gamma-\ln(-i\alpha_2)], \quad \text{(A28)}$$

$$\tilde{J}_0(\alpha_1,\alpha_2)=-i\alpha_1[1-\gamma-\ln(-i\alpha_1)] \\ +i\alpha_2[1-\gamma-\ln(i\alpha_2)], \quad \text{(A29)}$$

and

$$\phi_1(\alpha_1,\alpha_2)=-i[2\gamma+\ln(i\alpha_1)+\ln(-i\alpha_2)], \quad \text{(A30)}$$

$$\phi_0(\alpha_1,\alpha_2)=i[2\gamma+\ln(-i\alpha_1)+\ln(i\alpha_2)], \quad \text{(A31)}$$

where we assume the usual definition of the logarithmic function with a cut along the real negative axis.

Similarly as was done in [13] for the sum $\tilde{J}_1(\alpha)+\tilde{J}_0(\alpha)$ one can also obtain higher-order terms of the expansions of $\tilde{J}_\sigma(\alpha)$ in power of α. Both functions $\tilde{J}_1$ and $\tilde{J}_0$ given by Eqs. (A17) and (A18) contain terms proportional to $\ln(\alpha_1+\alpha_2)$ but one can check by direct series expansions that in the corresponding sums these terms all cancel and the only logarithmic contributions to these functions are the ones presented in Eqs. (A24) and (A25), as it should be to ensure the analytical properties of $\tilde{J}_\sigma(\alpha)$.

[1] C. E. Porter, *Statistical Theories of Spectra: Fluctuations* (Academic Press, New York, 1965)

[2] M. L. Mehta, *Random Matrix Theory* (Springer, New York, 1990).

[3] O. Bohigas, in *Chaos and Quantum Mechanics*, edited by M.-J. Giannoni, A. Voros, and Z. Zinn-Justin, Les Houches Summer School Lectures LII, 1989 (North Holland, Amsterdam, 1991), p. 87.

[4] M.V. Berry and M. Tabor, Proc. R. Soc. London, Ser. A **349**, 101 (1976); J. Phys. A **10**, 371 (1977).

[5] O. Bohigas, M.-J. Giannoni, and C. Schmit, Phys. Rev. Lett. **52**, 1 (1984).

[6] J. Marklof, Commun. Math. Phys. **199**, 169 (1998).
[7] A.V. Andreev *et al.*, Phys. Rev. Lett. **75**, 2304 (1995).
[8] A.V. Andreev and B.L. Altshuler, Phys. Rev. Lett. **75**, 902 (1995).
[9] O. Agam, B.L. Altshuler, and A.V. Andreev, Phys. Rev. Lett. **75**, 4389 (1995).
[10] E.B. Bogomolny and J.P. Keating, Phys. Rev. Lett. **77**, 1472 (1996).
[11] B.I. Shklovskii *et al.*, Phys. Rev. B **47**, 11 487 (1993).
[12] E. Bogomolny, U. Gerland, and C. Schmit, Eur. Phys. J. B **19**, 121 (2001).
[13] E. Bogomolny, U. Gerland, and C. Schmit, Phys. Rev. E **63**, 036206 (2001).
[14] E. Bogomolny, U. Gerland, and C. Schmit, Phys. Rev. E **59**, R1315 (1999).
[15] M. Gaudin, Nucl. Phys. **85**, 545 (1966); P.J. Forrester, Phys. Lett. A **173**, 355 (1993).
[16] S. Albeverio, F. Gesztesy, R. Høegh-Krohn, and H. Holden, *Solvable Models in Quantum Mechanics* (Springer, New York, 1988).
[17] P. Šeba, Phys. Rev. Lett. **64**, 1855 (1990).
[18] G. Berkolaiko, E.B. Bogomolny, and J.P. Keating, J. Phys. A **34**, 335 (2001).
[19] M. Sieber, J. Phys. A **32**, 7679 (1999).
[20] I.L. Aleiner and K.A. Matveev, Phys. Rev. Lett. **80**, 814 (1998).
[21] E.B. Bogomolny, P. Leboeuf, and C. Schmit, Phys. Rev. Lett. **85**, 2486 (2000).
[22] T. Jonckheere, B. Gremaud, and D. Delande, Phys. Rev. Lett. **81**, 2442 (1998).
[23] H. Bateman and A. Erdélyi, *Higher Transcendental Functions* (McGraw-Hill, New York, 1953), Vol. II.